Available online at www.sciencedirect.com
SCIENCE DIRECT
Catalysis Today 102–103 (2005) 45–49
CATALYSIS TODAY
www.elsevier.com/locate/cattod

# Carbon nanofiber supported Ni catalyst: Effects of nanostructure of supports and catalyst preparation

Esther Ochoa-Fernández [a], De Chen [a,*], Zhixin Yu [a], Bård Tøtdal [b], Magnus Rønning [a], Anders Holmen [a]

[a] Department of Chemical Engineering, Norwegian University of Science and Technology (NTNU), Sem Sælandsvei 4, N-7491 Trondheim, Norway
[b] Department of Physics, Norwegian University of Science and Technology (NTNU), Sem Sælandsvei 4, N-7491 Trondheim, Norway

Available online 25 March 2005

**Abstract**

Carbon nanofibers (CNFs) have been used as templates for manipulating the properties of Ni catalyst particles. Both incipient wetness impregnation and deposition–precipitation have been used to prepare the catalysts. Relatively well-dispersed Ni nanoparticles have been prepared on oxidised CNFs by incipient wetness impregnation. The diameter of the CNFs has been shown to have a significant effect in determining the Ni crystal size. In addition, CNFs are suitable templates to induce microstrain to metal particles. Such microstrain has significant effects on the activity of Ni crystals during ethane hydrogenolysis. This provides new opportunities to manipulate the crystal size and activity of the metal by selecting proper carbon nanofibers as support. TPO has been demonstrated as a powerful tool to study the CNF supported catalyst and to provide information on Ni loading and relative activity of NiO for CNF oxidation.


*Keywords:* Carbon nanofibers; Ni catalyst; Ni nanoparticles; Ethane hydrogenolysis

## 1. Introduction

Carbon nanofibers (CNFs) have many interesting properties, resulting in a wide range of applications such as catalyst supports, selective adsorption/absorption agents, energy storage (including hydrogen and power battery), composite materials, nano-electric and nano-mechanical devices, as well as field emission devices [1,2].

CNFs have been considered as promising alternative support materials because of their special properties. CNFs present high mechanical strength, chemical inertness, and they can be used both in acidic and basic solutions. It is relatively easy to use combustion for recovery of the precious metal after deactivation of the catalysts. Furthermore, the structure and porosity can be tuned by synthesis conditions, CNFs are chemically pure, and the surface properties can be controlled by surface oxidation [3]. A variety of metal catalysts have been prepared on CNF supports and tested in hydrogenation reactions [4–10].

The present work deals with an investigation of the preparation and characterisation of CNF supported Ni catalyst. Incipient wetness and deposition–precipitation procedures are compared and the influence of the pre-oxidation of the fibers is also reported. Special attention has been given to develop temperature-programmed oxidation as a simple tool for a fast evaluation of Ni catalyst supported on CNF. The TPO results are related with the turnover frequency (TOF) for the hydrogenolysis of ethane. A detailed TEM analysis of the deposited Ni particles has been performed. TEM examination provides not only direct information of particle size, but also the size distribution over a certain range.

## 2. Experimental

Three types of CNF support materials have been prepared in our laboratory: platelet (Pl), carbon filament (CF) and herring-bone (HB) [7]. CNF supported nickel catalysts (12.5 wt.% Ni) were prepared by both incipient wetness impregnation (IW) and deposition–precipitation (DP) of

* Corresponding author.
*E-mail address:* chen@chemeng.ntnu.no (D. Chen).

0920-5861/$ – see front matter © 2005 Elsevier B.V. All rights reserved.
doi:10.1016/j.cattod.2005.02.005

nickel nitrate ($Ni(NO_3)_2{\cdot}6H_2O$) onto the three types of nanofibers. The CNFs were previously treated for 3 days in a 1 M HCl solution in order to remove impurities. A fraction of HB supports were oxidised by boiling in a $HNO_3$ (65%) solution for 10 min for studying effects of the surface modification of CNFs.

Temperature programmed oxidation (TPO) measurements of the supports and prepared Ni/CNF catalysts were carried out under air-flow (80 ml $min^{-1}$) in a Thermogravimetric Analyser (Perkin-Elmer). The temperature was increased from room temperature to 1253 K at a heating rate of 10 K $min^{-1}$. The TEM investigation was performed on a JEOL 2010F transmission electron microscope. The TEM samples were prepared by dispersing nanofibers in ethanol by ultrasonication and then depositing a few drops onto a copper grid. XRD spectra were recorded on a Siemens diffractometer (D500) using monochromatic radiation. Analysis of the experimental spectra for the crystal size determination was performed in two steps. Firstly, the experimental XRD peaks were simulated by means of the software *Profile* [11], where several models can be selected to fit the experimental data. Secondly, the program *Wincrysize* [12] was used to estimate the crystallite size and microstrain. Hydrogen chemisorption measurements were performed on a Micromeritics ASAP 2010C V2.01 apparatus. The $H_2$ adsorption isotherms were measured at 308 K. Ethane hydrogenolysis has been used as a probe reaction in the present work to test the catalytic activities of Ni nanoparticles. The reaction was carried out in a vertical flow reactor system connected to a mass spectrometer. Details about CNFs synthesis, catalyst preparation and further characterisation have been reported earlier [7].

## 3. Results and discussion

TPO experiments have been found to be an efficient tool to evaluate the CNF-supported catalyst and to provide information on Ni loading and relative activity of NiO for CNF oxidation. The Ni loading measured by TPO on most of the catalysts are close to the nominal value 12.5 wt.%. The Ni loading has been calculated as a function of the difference between the remaining weight of the catalyst and the support after complete oxidation of the carbon. Fig. 1(a) shows a typical TPO profile of CNF support and supported NiO prepared by both IW and DP. Selected properties of the different catalysts are listed in Table 1. The results clearly indicate that both the CNF structure and the preparation method have pronounced effects on the catalysts properties. Better control of the metal loading is reached by IW preparation, where the nickel loading established by thermogravimetric analysis are closer to the nominal value than for the catalyst prepared by DP. The dispersion measured by chemisorption ranges from 1% to 2.5% depending on the nanostructure of CNFs and the catalyst preparation. The Ni dispersion for DP was in general equal

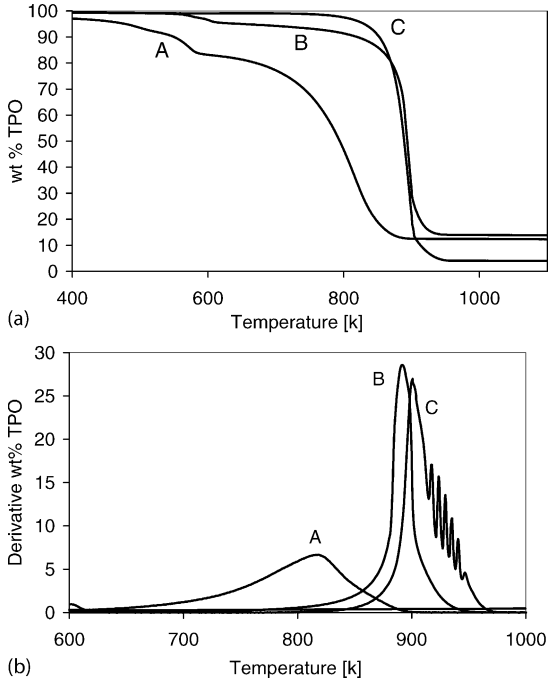


Fig. 1. (a) TPO and (b) TPO derivative profiles: (A) CF IW, (B) CF DP and (C) CF support. Heating rate: 10 K $min^{-1}$, air-flow: 80 ml $min^{-1}$.

Table 1
Properties of Ni catalyst supported on CNF and their activation energy for ethane hydrogenolysis

| Catalyst | Ni loading (wt.%) | Dispersion[a] (%) | Strain ($\times 10^2$) | $E_a$ (kJ/mol) |
|---|---|---|---|---|
| Carbon filament IW | 10.81 | 1.61 | 2.38 | 102.2 |
| Carbon filament DP | 8.67 | 2.13 | 3.26 | 105.0 |
| Platelet DP | 12.53 | 0.77 | 2.57 | 112.3 |
| Herring-bone IW | 11.19 | 1.53 | 0.51 | 101.5 |
| Herring-bone ox. IW | 11.50 | 2.39 | 0.19 | 103.2 |
| Herring-bone ox. DP | 8.17 | 2.39 | 3.31 | 76.2 |

[a] From $H_2$-chemisorption.

to or higher than that for the corresponding IW catalyst. However, the XRD measurements indicate that the DP method yields larger Ni particles than IW, which is in good agreement with the TEM observation as reported previously [7]. It should be noted that these DP results are in contrast to the observation reported by Bitter et al. [13]. DP obtained highly dispersed and highly loaded Ni nanocrystals on CNF in their investigation. This may be due to a difference in the oxidation conditions, since Bitter et al. [13] used a much stronger oxidant and a longer reflux time. The concentration of surface functional groups seems to be an important factor for the deposition–precipitation method.

As mentioned above, TPO experiments provide information about the relative activity of the catalysts. The derivatives of the TPO profiles for the CF support and the catalysts prepared by incipient wetness and deposition–precipitation are plotted in Fig. 1(b). The CF support has an

onset temperature for bulk oxidation at approximately 850 K. For CF DP and CF IW the bulk oxidation starts at about 800 K and 600 K, respectively. The maximum rate of oxidation is observed at 900 K, 892 K ad 823 K in each case. The difference between the temperature for the maximum rate of oxidation between the support and the different catalysts ($\Delta T$) gives an indication about the relative catalytic activity of NiO for CNF oxidation. Accordingly, the catalyst made from CF support prepared by IW ($\Delta T$ = 77 K) displays higher activity than the catalyst prepared by DP ($\Delta T$ = 8 K) for the CNF oxidation. In general, the results show that the carbon nanostructure has significant effect on the catalytic activity. NiO on the herringbone support shows the highest activity, which is slightly favoured by the previous oxidation of the support. The activity of the NiO particles depends also significantly on the preparation method. Ni/CNFs prepared by IW exhibited higher activity than the catalysts prepared by DP. Fig. 2 shows that this activity is highly correlated with the deposited Ni crystal size and small crystals favour the carbon oxidation.

The activity of Ni nanoparticles has been tested for the hydrogenolysis of ethane. The carbon nanostructure and preparation method have also a pronounced effect on the activity for the ethane hydrogenolysis. According to Fig. 3(a) Ni/CNFs prepared by DP exhibited higher activity than the catalysts prepared by IW, even though the latter have smaller Ni particle size as measured by XRD. Ni on carbon filaments shows the highest catalytic activity while Pl DP catalyst has the lowest activity. The large diameter of the platelet fibers (∼150 nm) and less curvature compared to herring-bone and carbon filaments leads to less strain in the metal particles. This factor together with the low dispersion is suggested to be the reason of the lower detected activity and higher activation energy (112 kJ/mol). The activation energy for all catalysts is in the range of 102–113 kJ/mol, with exception of the HB ox. DP (76 kJ/mol) as presented in Table 1. This level is similar to that obtained by Lomot et al. [14] and lower than the activation energies reported by Sinfelt et al. (125 kJ/mol [15]). The lower activation energy of the HB ox. DP can also be explained by the higher dispersion and larger strain of this catalyst.

Regarding the stability of the catalysts, the results show that there is no hysteresis detected in the activities of Ni/CNFs, as shown in Fig. 3(b). Accordingly, there is no indication of changes in the Ni nanocrystals after the measurements.

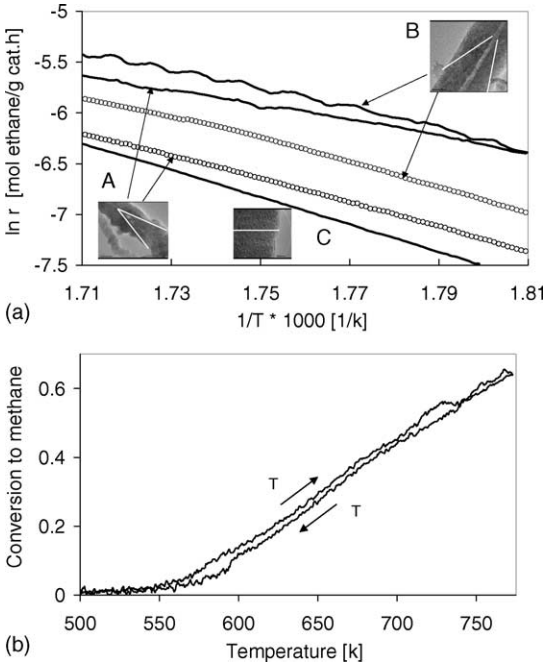


Fig. 3. (a) Arrhenius plots for the hydrogenolysis of ethane on Ni supported on: (A) herring-bone, (B) carbon filament and (C) platelet, prepared by: (◯) incipient-wetness (—) deposition–precipitation. (b) Activity measured during temperature scans (up and down) for the CF DP catalyst. The catalysts were heated at a rate of 3 K $min^{-1}$ from 473 K to 773 K before lowering the temperature to 473 K in a mixture of $C_2H_6/H_2$/Ar (10/12/78 ml $min^{-1}$).

A relation between activity detected by means of TPO and the TOF for the hydrogenolysis of ethane has been observed, as shown in Fig. 4. Catalysts that present higher activity for the oxidation of carbon are the least kinetically favoured for the hydrogenolysis of ethane. According to Figs. 3 and 4, larger crystals favour the TOF for the hydrogenolysis of ethane. Che and Bennett [16] have reviewed the effects of crystal size on the catalytic properties of supported metals for different reactions. These authors found an optimised Ni crystal size for the ethane hydrogenolysis of about 3 nm and further increase in

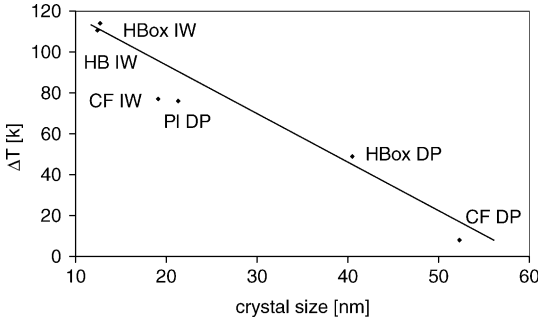


Fig. 2. Dependence of the carbon oxidation activity on the Ni crystal size measured by XRD.

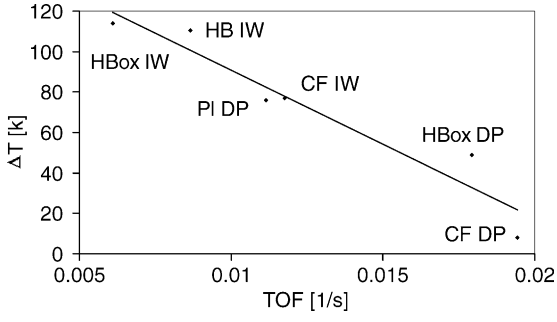


Fig. 4. Relation between activity (detected by means of TPO) and TOF for the hydrogenolysis of ethane of the catalyst at 563 K.

crystal size reduced the TOF. However, our catalysts behave very differently. This phenomenon may be explained by the microstrain detected in the catalyst. CNFs have been demonstrated to be good templates for inducing microstrain to metal particles [7]. Such microstrain has been shown to significantly modify the chemisorption properties of the metal [17]. This effect is due to shifts in the metal d bands induced by the stress [18]. As a result, the induced microstrain modifies the ability of a surface to form bonds to adsorbed atoms or molecules. The present study confirms that the effect of the strain on the CNF oxidation and ethane hydrogenolysis activity follow different trends as shown in Fig. 5. An increase in the average microstrain to a certain level in the nickel particles supported on the different CNFs leads to higher turnover frequencies for ethane hydrogenolysis. A further increase in lattice expansion above this level lower the activity and hence a maximum TOF is found at moderate microstrain values. In contrast, the induced microstrain decreases the activity for the oxidation of carbon. This indicates that shift in d bond in Ni crystals has different effects on different reactions.

TEM images of well-dispersed Ni nanoparticles deposited on oxidised CNFs with different diameters are presented in Fig. 6. The size distributions for each fiber plotted in Fig. 7 were obtained by counting the single particles. It should be

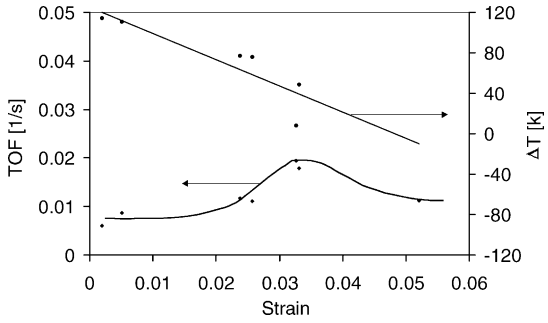


Fig. 5. Strain effect on the carbon oxidation and hydrogenolysis activity of the catalyst at 563 K. Other conditions identical as stated in Fig. 3(b).

pointed out that particles with sizes smaller than 2 nm are difficult to detect due to resolution limits and are therefore not included in the crystal size distribution profiles. Fig. 7 shows that the diameter of the CNFs plays a significant role in determining Ni crystal size. Small Ni crystals with narrow distribution can be obtained on the CNFs with small diameter. As a result, the average metal particle size can be controlled by means of the CNF diameter. It should be noted that the average crystal size obtained for this catalyst by TEM (13–14 nm) is in good agreement with the XRD data (12.7 nm).

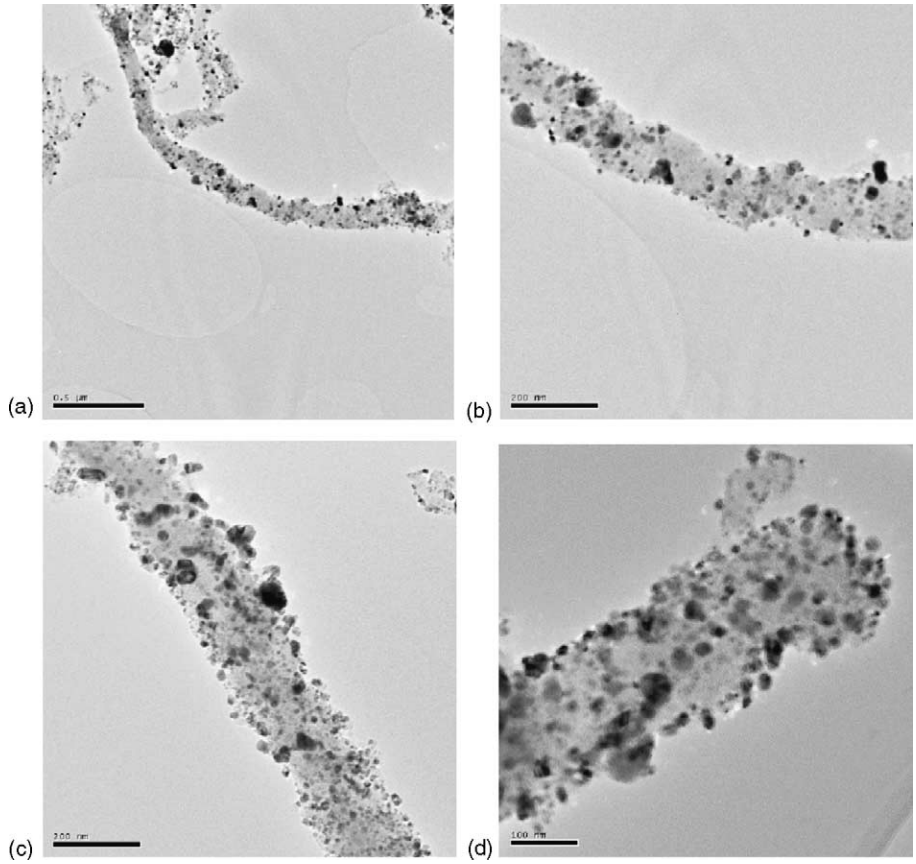


Fig. 6. TEM images of Ni particles on oxidised herring-bone CNFs prepared by IW. Fiber diameter around: (a) 50 nm, (b) 100 nm, (c) 150 nm and (d) 200 nm.

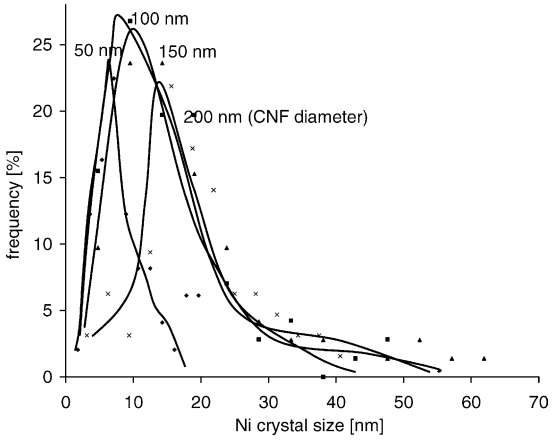


Fig. 7. Dependence of Ni crystal size distribution on CNF diameter.

## 4. Conclusion

The present work shows that CNFs serve as templates for Ni nanoparticles. The template effects lead to a strong size dependence of the CNF diameter for the Ni particles and introduce high microstrain due to the surface curvature of CNFs. As a result, the average metal particle size and distribution can be controlled by means of the CNF diameter. In addition, strain creates a concurrent up-shift of the metal d states significantly affecting the activity of Ni during ethane hydrogenolysis and carbon oxidation. Temperature programmed oxidation has been demonstrated to be a very simple and efficient tool to give an initial evaluation of the catalytic activity and metal loading.

## Acknowledgement

The Research Council of Norway is thanked for financial support.

## References

[1] K.P. de Jong, J.W. Geus, Catal. Rev. -Sci. Eng. 42 (2001) 481.
[2] F. Salman, C. Park, R.T.K. Baker, Catal. Today 53 (1999) 38.
[3] M.L. Brandl, J.M.P. van Heeswijk, J.H. Bitter, A.J. van Dillen, K.P. de Jong, Carbon 42 (2004) 307.
[4] T.G. Ros, A.J. van Dillen, J.W. Geus, D.C. Koningsberger, Chem. Eur. J. 8 (13) (2002) 2868.
[5] T.G. Ros, D.E. Keller, A.J. van Dillen, J.W. Geus, D.C. Koningsberger, J. Catal. 211 (2002) 85.
[6] M.S. Hoogenraad, M.F. Onwezen, A.J. van Dillen, J.W. Geus, Stud. Surf. Sci. Catal. 101 (1996) 1331.
[7] E. Ochoa-Fernández, D. Chen, Z. Yu, B. Tøtdal, M. Rønning, A. Holmen, Surf. Sci. Lett. 554 (2004) 107.
[8] A. Chambers, T. Nemes, N.M. Rodriguez, R.T.K. Baker, J. Phys. Chem. B 102 (1998) 2251.
[9] C. Park, R.T.K. Baker, J. Phys. Chem. B 102 (1998) 5168.
[10] C. Park, R.T.K. Baker, J. Phys. Chem. B 103 (1999) 2453.
[11] Diffracplus Profile, Profile fitting program, User's Manual, Siemens.
[12] Diffracplus Win-crysize, Crystallite size and microstrain, User's Manual, Bruker Analytical X-Ray Systems.
[13] J.H. Bitter, M.K. van der Lee, A.G.T. Slotboom, A.J. van Dillen, K.P. de Jong, Catal. Lett. 89 (2003) 139.
[14] D. Lomot, W. Juszczyk, Z. Karpinski, R. Larsson, J. Mol. Catal. A: Chem. 186 (2002) 163.
[15] J.H. Sinfelt, W.F. Taylor, D.J.C. Yates, J. Phys. Chem. 69 (1966) 95.
[16] M. Che, C.O. Bennett, Adv. Catal. 36 (1989) 55.
[17] M. Gsell, P. Jakov, D. Menzel, Science 280 (1998) 717.
[18] M. Mavrikakis, B. Hammer, J.K. Nørskov, Phys. Rev. Lett. 81 (1998) 2819.